GEOLOGICAL SURVEY OF CANADA

DEPARTMENT OF MINES AND TECHNICAL SURVEYS

PAPER 63-42

GEOCHEMISTRY OF THE DAWSON SETTLEMENT BOG MANGANESE DEPOSIT, NEW BRUNSWICK

(Report and 7 figures)

A. C. Brown

Price 35 cents

1964

GEOLOGICAL SURVEY

OF CANADA

PAPER 63-42

GEOCHEMISTRY OF THE DAWSON SETTLEMENT BOG MANGANESE DEPOSIT, NEW BRUNSWICK

By

A.C. Brown

D E P A R T M E N T O F

M I N E S A N D T E C H N I C A L S U R V E Y S

C A N A D A

CONTENTS

Appendices

Illustrations

INTRODUCTION

A study of the major chemical systems existing in the Dawson Settlement manganese bog was undertaken by the writer while employed by the Geological Survey during the 1961 field season. The bog is located on the south slope of the Hopper Creek valley, 1 1/2 miles southeast of Dawson Settlement, and 10 miles south of Moncton, New Brunswick.

The obvious precipitation of iron at the orifices of bog springs, and deposition of manganese downstream from the orifices after mixing of the water with the atmosphere, suggests an Eh-pH control of the chemical processes. The source of the iron and manganese is not definitely known, but it is probably in the lower Windsor limestone, which is noted for its manganese oxide occurrences in a belt extending 40 miles to the southwest. Outcrops in the immediate area are lacking, but Windsor limestone is found 1 mile southeast of the Dawson Settlement bogs.

Acknowledgments

The writer is indebted to A.Y. Smith, and to J.G. Cassils, P.B. Robertson, and A.L. Sangster for assistance in the field. Particular thanks are due to Dr. J.R. Kramer of the University of Western Ontario for guidance during the laboratory studies; to Dr. G.M. Boone, also of the University of Western Ontario, for assistance in the X-ray studies; and to Dr. Norman Good of the Pesticide Research Institute, Department of Agriculture, London, Ontario, who ran paper chromatographs.

Nature of the Bog

The Dawson Settlement bog manganese or wad deposits occur in two adjacent bogs, which were drained for mining operations during 1887 to 1930. The writer examined only the western bog and observed a total of seven spring orifices (see Fig. 1). One spring (location 10) is presently forming a typical wet bog of black, manganiferous muck, while the other springs are drained by trenches. No precipitates are being deposited from the springs at locations 5, 11, and 12, but iron is precipitating from a line of springs at the 95-foot contour above Hopper Creek (locations 4, 6, and 7). Manganese is precipitating downstream from locations 4 and 7, after all obvious iron has been deposited, but the locality at which manganese first precipitates is not apparent; it is definitely precipitating at locations 1, 2, 3, and 9.

FIELD PROCEDURES

Eh and pH readings were made in situ at locations 1 through 10 on a Beckman Model N-2 pH-meter using platinum and glass electrodes respectively, coupled with a saturated calomel reference electrode. The instrument was standardized against pH 7 buffer, and the temperature was compensated to that of the spring water. A steel rod was used to support the electrodes to obtain stable readings. Stability was rapidly established during pH readings and during Eh readings of the bottom muck. Eh readings of the water drifted as little as 0 m.v. in one case, to as much as +54 m.v. and -45 m.v. in other cases before reaching reasonable stability. Eh was recorded every minute until three identical readings were obtained. Generally fifteen minutes was sufficient for this purpose; time did not permit longer runs.

Alkalinity was determined in the field by recording the pH before and after the addition of measured volumes of 0.01 N HCl to 20 ml. of sample water. The alkalinity is the number of equivalents of free hydrogen ions, which, added to the sample, react to form weakly dissociated ions:

$$\text{i.e., Alkalinity} = \frac{(HiVs + NVa) - Hf\,(Vs + Va)}{Vs} \text{ equivalents/litre,}$$

where Hi is the initial hydrogen ion concentration, Hf is the final hydrogen ion concentration, Vs is the volume of sample in ml., Va is the volume of acid, and N is the normality of the acid. The term HiVs may be neglected since Hi is negligible ($< 10^{-6}$) compared to the other terms when Hf is large.

Water samples for chemical and semi-quantitative spectrographic analyses were collected in polyethylene bottles, which were rinsed, filled with water excluding all air, and tightly sealed. In addition, water samples for immediate copper-lead-zinc analyses, and samples of saturated bog material from the bottom of all locations were collected and sealed in polyethylene bags.

LABORATORY ANALYSES AND RESULTS

Water Analyses

Analyses of water for Cu^{+2}, Pb^{+2}, and Zn^{+2} were made by the writer in a mobile laboratory using standard colorimetric methods with dithizone (diphenylthiocarbazone) (Boyle, Illsky, and Green, 1955)[1] as reagent. The sensitivity using 100 ml. samples is 0.005 p.p.m. None of these metals was detected in samples from locations 1 through 10.

---

[1] Names and/or dates in parentheses refer to publications listed in the References.

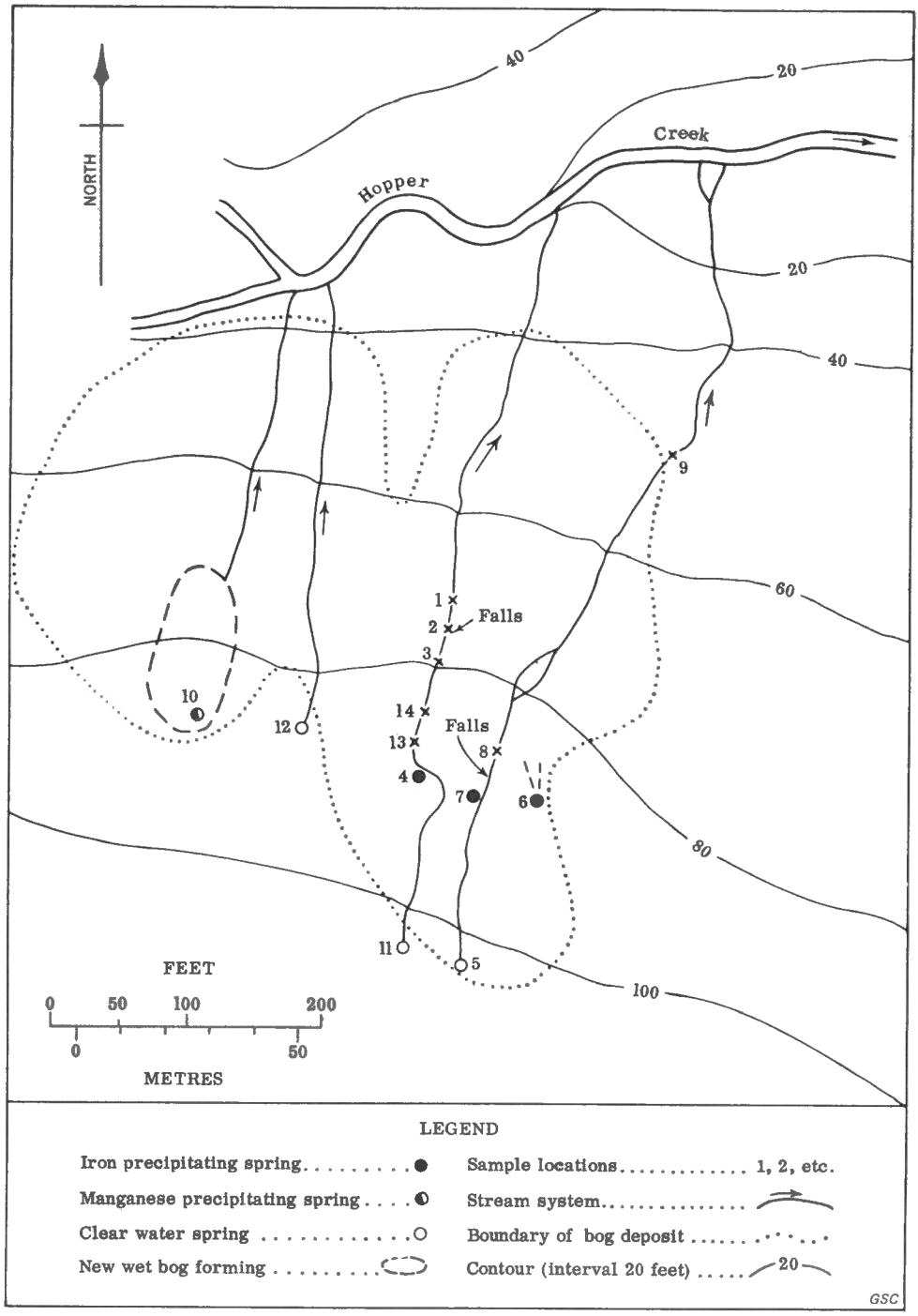

Figure 1. Plan of manganese bog, Dawson Settlement, showing locations of samples

Water samples were also chemically analyzed by the Industrial Waters Section, Mines Branch, Ottawa (see Table I) for Ca^{+2}, Mg^{+2}, Na^{+}, K^{+}, Fe^{+2}, Mn^{+2}, Al^{+3}, Ba^{+2}, CO_3^{-2}, HCO_3^{-}, SO_4^{-2}, Cl^{-}, F^{-}, PO_4^{-3}, NO_3^{-}, SiO_2, and NH_3. Standard procedures of the American Public Health Association and the American Society for Testing Materials were employed for these determinations. In addition, semi-quantitative spectrographic analyses for Fe, Al, Mn, Cu, Zn, Pb, Ba, B, Cr, Ni, Ag, Sr, Ti, and Zr were made on the residue of the water after evaporation (Table II). The major ionic species in moles per litre are given in Table III, which also includes field readings of pH, Eh, alkalinity, and temperature.

Eh and pH readings (see Table IV) were made on water saturated bog samples, which had been stored free from the atmosphere for six months in polyethylene bags. It is assumed that equilibrium between solid and aqueous phases had been attained in this time. Water was extracted from these samples for determination of total iron and manganese in solution. Iron analyses were made using 4:7-diphenyl-1:10-phenanthroline as reagent (Smith, McCurdy, and Diehl, 1952), and manganese analyses were made using the permanganate method (Sandell, 1959). The sensitivity in both cases is 0.01 p.p.m. using 100 ml. samples. Neither element was detected. This was anticipated from the solubility product of ferric hydroxide and the equilibrium constants of manganese oxides; i.e., Ksp $Fe(OH)_3 = 6 \times 10^{-38}$ (Latimer, 1952), and K (Mn^{+2}, Mn^{+4}, MnO_2) = 2×10^{-42} (calculated at pH 7).

Bog Material

The determination of the composition of the bog material was attempted by X-ray powder diffraction methods. A cobalt target and iron filter were used with a glass capillary mount in a 1/2-radian camera. Length of exposure, amperage, and voltage were varied in order to obtain the optimum pattern. Fogging due to iron impurities was extensive, but faint lines were obtained with a six hour exposure at Ma = 12 and Kv = 20. No peaks were detectable with the diffractometer and scintillation detector. Four lines having d = 7.42, 3.86, 2.455, and 1.415 Å were measured.

Although these lines do not correspond to those of any recorded patterns of known iron, manganese, or other compounds, two lines compare favourably with the only two lines obtained by Smitheringale (1929) on wad from Conquerall, Nova Scotia (d = 2.45, and 1.40). The chemical composition given by the ASTM card file for Smitheringale's wad mineral was $MnO_2 \cdot (0\text{-}1)\ MnO \cdot nH_2O$. However, this card was withdrawn from the files in 1960 because of its incorrect chemical formula.

Table I

Chemical Analyses of Spring Water
(Concentrations in p.p.m.)

Sample Number	61-1	61-2	61-3	61-4	61-5	61-6	61-7	61-8	61-9
Location	1	2	3	4	5	6	7	9	10
Ca	25.7	26.3	27.1	32.8	1.7	32.7	35.3	22.6	28.3
Mg	2.2	1.2	2.8	2.0	1.2	1.7	1.8	1.6	1.9
Na	3.0	3.0	3.0	3.2	2.2	3.2	3.1	2.8	2.8
K	1.3	1.3	1.3	1.4	0.6	1.5	1.5	1.2	1.1
Fe (total)	0.22	0.14	0.35	1.47	0.04	3.3	2.0	0.78	0.14
Fe (dissolved)	0.01	Trace	0.04	0.06	0.01	0.34	0.02	0.01	0.01
Al	0.0	0.0	0.0	0.0	0.0	0.02	0.08	0.0	0.0
Mn (total)	0.06	0.03	0.04	1.1	0.01	1.2	1.1	0.12	0.49
Mn (dissolved)	Trace	Trace	0.04	0.95	0.01	1.2	1.1	0.05	0.01
Ba	< 0.1	<0.1	<0.1	<0.1	<0.1	<0.1			
CO_3	0.0	0.0	0.0	0.0	0.0	0.0	0.0	0.0	0.0
HCO_3	65.7	67.8	70.2	86.8	8.8	89.5	88.0	57.2	74.5
SO_4	19.6	19.6	19.3	23.7	4.5	24.8	24.7	16.8	19.3
Cl	2.0	2.4	1.6	2.2	1.9	2.1	2.8	2.4	2.7
F	0.09	0.09	0.09	0.1	0.03	0.08	0.12	0.12	0.12
PO_4 (total)	0.35	0.57	< 0.1	0.13	1.0	< 0.1	0.13	<0.1	<0.1
PO_4 (dissolved)	<0.1	<0.1	<0.1	<0.1	<0.1	<0.1	<0.1	<0.1	<0.1
NO_3	0.2	0.5	0.1	0.5	0.1	0.1	0.0	0.0	0.1
SiO_2	15	15	15	17	9.3	17	16	14	13
NH_3	0.2	0.2	0.2	0.2	0.0	0.1	0.0	0.0	0.0
Error in cation-anion balance.	+1.3	+0.3	+2.1	+0.9	-0.4	+1.2	+0.7	+0.8	-0.05

Analyses by Industrial Waters Section, Mines Branch,
Department of Mines and Technical Surveys.

Table II

Semi-Quantitative Spectrographic Analyses

of Residue from Spring Water after Evaporation

(Concentrations in p.p.m.)

Sample Number	61-1	61-2	61-3	61-4	61-5	61-6	61-7	61-8	61-9
Location	1	2	3	4	5	6	7	9	10
Fe	400	400	400	100	3000	1000	600	800	500
Al	200	100	100	300	1000	200	100	300	200
Mn	100	60	400	2000	100	1000	1000	30	100
Cu	70	70	100	70	100	20	300	100	100
Zn	**	**	Trace	**	900	700	Trace	200	200
Pb	200	100	200	100	200	100	100	500	300
Ba	400	300	200	300	700	200	300	200	400
B	20	20	20	20	200	30	20	20	30
Cr	Trace	20	10	50	40	10	50	20	20
Ni	10	Trace	100	100	80	100	300	200	4
Ag	1	2	3	2	2	3	30	1	4
Sr	300	Trace	Trace	400	300	300	70	60	300
Ti	10	Trace	6	30	80	6	4	4	6
Zr	**	**	**	**	30	**	**	**	**

Analyses by Spectrographic Laboratory, Mines Branch, Department of Mines and Technical Surveys.

Table III

Major Physical and Chemical Properties of the Spring Water

Sample GSC# SM	61-1	61-2	61-3	61-4	61-5	61-6	61-7	----	61-8	61-9
Location (Fig. 1)	1	2	3	4	5	6	7	8	9	10
Temperature (°C)	10.5	10.0	10.0	7.0	9.0	7.0	6.0	8.0	13.0	7.0
pH	7.75	7.80	7.65	7.10	5.80	7.10	7.20	7.25	7.75	7.25
Eh (mv.) in situ Free Water	+408	+459	+404	+180	+539	+204	+162	+281	+418	+441
Bottom Muck	+639	+654	+582	+228	+569	+237	+195	+334	+536	+606
Alkalinity x 10^3 (equiv./litre)	1.00	1.18	1.24	1.48	0.48	1.47	1.48	0.99	1.04	1.32
Mn (total)* x 10^6	1.1	0.55	0.75	20.0	0.18	21.8	20.0	----	2.2	9.0
Fe (total)* x 10^6	3.9	2.5	6.3	26.3	0.71	59.1	35.8	----	14.0	2.5
Ca^{+2}* x 10^3	0.64	0.66	0.68	0.82	0.04	0.81	0.88	----	0.57	0.71
Mg^{+2}* x 10^3	0.09	0.05	0.12	0.08	0.05	0.07	0.07	----	0.07	0.08
Na^{+} * x 10^3	0.13	0.13	0.13	0.14	0.10	0.14	0.13	----	0.12	0.12
HCO_3^{-}* x 10^3	1.08	1.11	1.15	1.42	0.14	1.47	1.44	----	0.94	1.22
SO_4^{-2}* x 10^3	0.20	0.20	0.20	0.25	0.05	0.26	0.26	----	0.18	0.20

*Concentrations in moles per litre.

Table IV

Eh-pH Values of Bottom Muck

Stored Free of Air for Six Months

Location on Figure 1	Eh (mv.)	pH
1	+555	7.21
2	+596	6.95
3	+565	7.25
4	+95	7.10
6	+590	7.63
7	+474	7.87
8	+569	6.95
9	+582	7.20
10	+627	6.80
13	+505	6.95
14	+445	7.35

The writer's bog material, however, is probably a complex of hydrated divalent and tetravalent manganese oxides existing in the amorphous state, possibly a mineral having the psilomelane structure. However, psilomelane, defined as a barium-bearing mineral, $BaMn^{+2}Mn_8^{+4}O_{16}(OH)_4$, is not a likely precipitate, because there is insufficient barium in the specimen (< 0.1 p.p.m.) for the amount of manganese removed from solution (~ 1.1 p.p.m.). Possibly other cations may proxy for barium. Unfortunately, thermodynamic data for psilomelane are not available.

Goldberg and Arrhenius (1958) described a double-layered structure of MnO_2 alternating with disordered layers of $Mn(OH)_2.xH_2O$ and $Fe(OH)_3.xH_2O$ as found by Buser and Grütter (1956, 1958) in marine manganese nodules. The ions of the disordered layer appear to be exchangeable, and at least minor amounts of other ions can proxy for manganous and ferric ions.

Relatively pure iron precipitates from the streams sampled by the writer also gave no detectable peaks on examination by X-ray powder diffraction methods. Indeed, background intensity was more uniform than in the case of manganese oxides. Consequently, further X-ray studies were not attempted on iron samples.

The writer's results indicate that both iron and manganese precipitate and exist in amorphous forms for the most part, although there is a slight degree of orientation indicated in the manganese oxide(s). These results are typical of those obtained in the precipitation of iron under surface conditions and of wad deposits (Hanson, 1932; Palache, Berman, and Frondel, 1944).

Organic Constituents

Analyses for the presence of common amino acids in the bog samples were made through the courtesy of the Pesticide Research Institute, London, Ontario, for the purpose of detecting a possible organic mechanism for the precipitation of iron and manganese, as has been postulated by several authors, including Zapffe (1931), Savage (1936), Palache, Berman, and Frondel (1944), and Krauskopf (1957). Indications of the amino acids, glycine, DL-aspercine, DL-leucine, and DL-tryptophan were not found, using paper chromatographic methods. However, these results do not eliminate the possibility of precipitation of iron and manganese by means of other organic constituents.

CHEMISTRY OF IRON-MANGANESE DEPOSITION

Iron and manganese are probably carried in solution as the reduced ions, Fe^{+2} and Mn^{+2}. Possibly the manganous ion is complexed with bicarbonate and sulphate ions, but the effect is negligible at the low concentrations of Mn^{+2}, HCO_3^-, and SO_4^{-2} encountered. For example, Goldberg and Arrhenius (1958) found that at least 85 per cent of the manganese in sea water exists in the true dissolved state, Mn^{+2}, at concentrations of manganese and bicarbonate of 4×10^{-8} and 5×10^{-4} moles per litre respectively.

The major chemical processes probably occurring in the spring water are shown in Figure 2. The importance of thorough mixing of the water with the air is shown by the essential part oxygen plays in the hydrolysis of iron and in the oxidation of manganese. The tetravalent oxide of manganese has been chosen for convenience only. Changes in the pH of the system are principally caused by dissociation of the bicarbonate ion during equilibration with CO_2 in the atmosphere. The precipitation of iron and manganese has a negligible effect on the pH owing to their low concentrations relative to the bicarbonate ion.

System HCO_3^- - $CO_2(l)$ - $CO_2(g)$ - H_2O

The spring water emerging at the surface is supersaturated with HCO_3^- with respect to atmospheric conditions, probably as a result of passing through the lower Windsor limestone. The P_{CO_2},

calculated from the measured alkalinity, pH, temperature, and ionic concentrations (see Appendix I), decreases consistently downstream from the spring orifices at locations 4 and 7, as shown in Table V. This loss of CO_2 to the atmosphere is in accordance with the lower P_{CO_2} of the normal atmosphere (4×10^{-4} atmospheres), and results in the shifting of the equation

$$HCO_3^- + H^+ = H_2O + CO_2$$

to the right. Any possible bicarbonate complexes of the metals Ca, Mg, and Mn then tend toward true dissolved species:

$$MHCO_3 = HCO_3^- + M^{+2}$$

$$HCO_3^- + H^+ = H_2O + CO_2,$$

(where M = Ca, Mg, or Mn).

Table V

Calculated P_{CO_2} at Given Locations

Location	Calculated P_{CO_2} (atmospheres)
1	9.40×10^{-4}
2	9.35×10^{-4}
3	14.3×10^{-4}
4	57.9×10^{-4}
5	404×10^{-4}
6	58.0×10^{-4}
7	45.5×10^{-4}
9	9.99×10^{-4}
10	37.3×10^{-4}

System Fe^{+2} - Fe^{+3} - $Fe(OH)_3$ - H_2O

On exposure of the spring water to the atmosphere, Fe^{+2} is oxidized to Fe^{+3}, which is then hydrolyzed to $Fe(OH)_3$:

$$Fe^{+2} = Fe^{+3} + e^-$$

$$Fe^{+3} + 3H_2O = Fe(OH)_3 + 3H^+$$

or,

$$Fe^{+2} + 3H_2O = Fe(OH)_3 + 3H^+ + e^-. \quad (1)$$

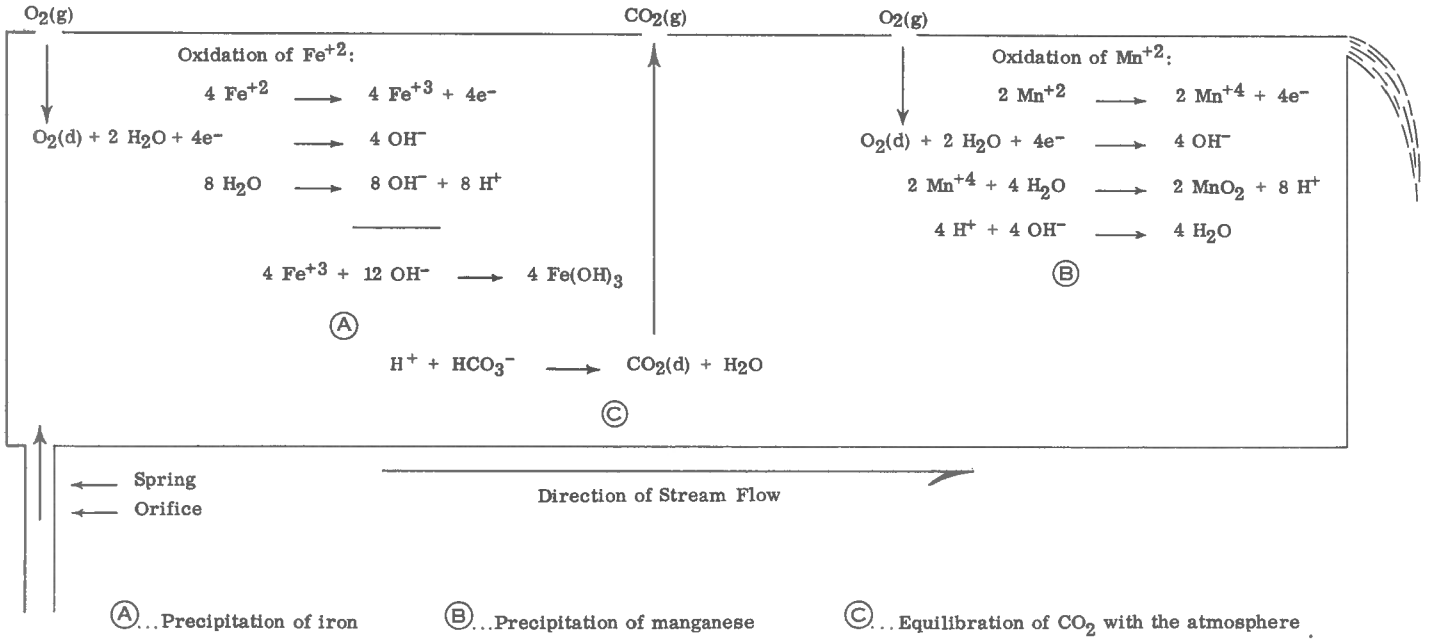

Note: Actual vertical depth of stream is negligible
Manganese oxide shown as MnO_2 for convenience only

Figure 2. Model of chemical processes in the stream systems

GSC

The redox potential for equation (1) is:

$$Eh = E^\circ + \frac{RT}{n\mathcal{F}} \ln \frac{(aH+)^3}{(a_{Fe}{}^{+2})},$$

where Eh is the redox potential in volts, $E^\circ = \frac{\Delta F}{n\mathcal{F}}$ is the redox potential under standard conditions, R is the gas constant, T is the absolute temperature, n is the number of electrons exchanged, $\mathcal{F}$ is the faraday, (a_M) is the activity of the ionic species M, and ΔF is the standard free energy of the reaction. New ΔF values corresponding to the water temperatures were calculated from the relation

$$\Delta F = \Delta H - T \Delta S,$$

assuming ΔH and ΔS do not vary with small temperature deviations from 25 °C (see Appendix II). Straight line graphs of Eh vs pH were then calculated for $(a_{Fe}{}^{+2}) = 2 \times 10^{-5}$ and 2×10^{-7} moles/litre, which covers the range of measured iron concentrations of the system (3.3 to 0.04 p.p.m.).

Figure 3 shows the plots of Eh vs pH for water samples from locations 1, 2, 3, 4, 5, 6, 7, 9, and 10. The springs precipitating iron (locations 4, 6, and 7) fall immediately within the stability field of $Fe(OH)_3$ for $(a_{Fe}{}^{+2}) = 2 \times 10^{-5}$ moles/litre while the other locations fall far to the right of the boundary for $(a_{Fe}{}^{+2}) = 10^{-7}$ moles/litre. Location 8, which marks the last trace of observed iron precipitate downstream from the orifice at location 7, is transitional in position between the plots of iron precipitate and manganese precipitate.

In all instances, the concentration of dissolved iron is greater than the stable concentration, and precipitation should occur. This is verified by the observation of iron precipitates at the spring orifices and for a few tens of feet downstream. Possibly minor amounts of iron are deposited further downstream, but the deposition of manganese obscures it. At location 10, where the Eh is high at the orifice, iron should either have precipitated before reaching the surface, possibly by mixing with aerated groundwater, or should precipitate simultaneously with manganese oxides.

Eh-pH readings of bottom muck in situ closely resemble those taken in free water at locations 4, 6, and 7 (Fig. 1). The stability of Eh readings made in the bottom muck appears to support the validity of these values, and the values obtained confirm that the iron precipitate is stable under the Eh-pH conditions existent at these locations.

Evidence that iron is not oxidized until exposed to the atmosphere was observed at location 7. The orifice was dug out, leaving a basin 1 foot deep, and the stream water from springs at higher elevations was dammed to one side. After two weeks, iron had precipitated as an ochrous deposit around the lip of the basin and

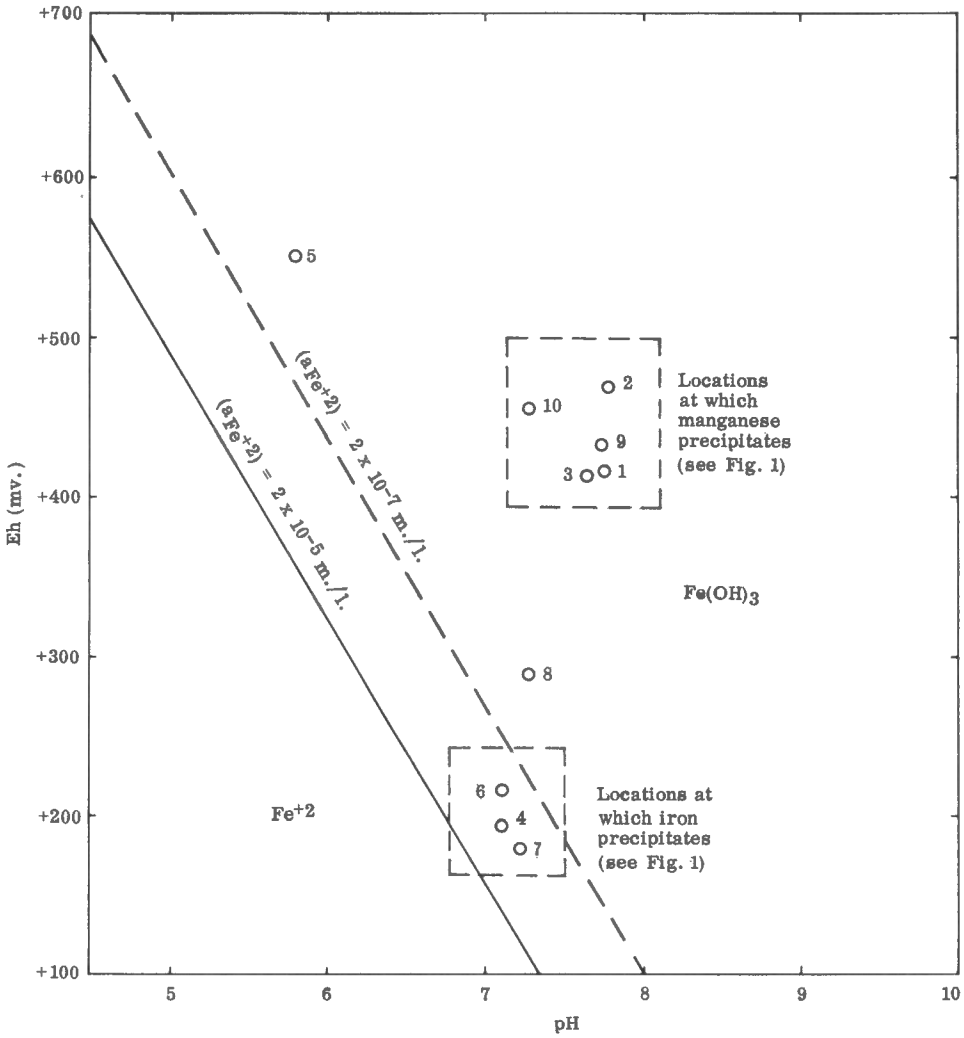

Location	$(a_{Fe^{+2}})$ m./l.	Location	$(a_{Fe^{+2}})$ m./l.
1	0.39×10^{-5}	6	6.00×10^{-5}
2	0.25×10^{-5}	7	3.60×10^{-5}
3	0.65×10^{-5}	8	—
4	2.60×10^{-5}	9	1.40×10^{-5}
5	0.07×10^{-5}	10	0.25×10^{-5}

Activities of Fe^{+2} for locations plotted above

GSC

Figure 3. Plot of Eh-pH values for free water with respect to the stability field of $Fe(OH)_3$ at 7°C

downstream from the spring, but no iron had been deposited in the deep parts of the basin where air circulation was non-existent. Therefore, a suitable redox potential for the stable formation of the iron precipitate is not attained until exposure of the spring water to the atmosphere.

Although the chemical composition of the iron precipitate was not determined, the conditions of the system are favourable for the formation and stable existence of $Fe(OH)_3$ at all locations if the water is in contact with the atmosphere. This factor, together with the physical appearance of the precipitate, strongly suggests that the iron is deposited as ferric hydroxide.

System Mn^{+2} - Mn oxide - H_2O

As the spring water flows downstream, the Eh of the system increases rapidly, and conditions suitable for the oxidation and precipitation of manganese are attained. Although the Eh observed is far less than the theoretical values for a system open to the atmosphere (Eh = 1.22 - 0.06 pH), Garrels (1960) has explained that such systems generally show much weaker "irreversible oxidation potentials" (e.g., Eh = 0.70 - 0.06 pH, or at pH 8, Eh = 0.22 volts). That the Eh values measured downstream (between 0.40 and 0.50 volts) exceed the "irreversible potential" may be attributed to the direct influence of free oxygen in contact with the platinum electrode. Such is the case at location 2, which is intermediate to locations 1 and 3 in position along the stream, but is located directly beneath a 4-foot waterfall. Consequently it shows a high Eh value due to vigorous aeration.

The manganous ion, Mn^{+2}, is oxidized to a very insoluble black manganese oxide. As the chemistry of wad minerals is not well known, the system Mn^{+2} - MnO_2 - Mn_2O_3- H_2O will be considered only as an approximation to the actual system:

i.e., $Mn^{+2} = Mn^{+4} + 2e^-$

$Mn^{+4} + 2\,H_2O = MnO_2 + 4H^+$

or $Mn^{+2} + 2\,H_2O = MnO_2 + 4\,H^+ + 2e^-$. (2)

Similarly,

$2\,Mn^{+2} + 3\,H_2O = Mn_2O_3 + 6\,H^+ + 2e^-$. (3)

Then, for equation (2),

$$Eh = E^\circ + \frac{RT}{2\mathcal{F}} \ln \frac{(aH^+)^4}{(a_{Mn^{+2}})},$$

and for equation (3),

$$Eh = E^\circ + \frac{RT}{2\mathcal{F}} \ln \frac{(a_{H^+})^6}{(a_{Mn^{+2}})^2}.$$

The Eh-pH stability fields for Mn^{+2} with MnO_2 and Mn_2O_3 were calculated at 10°C for $(a_{Mn^{+2}}) = 2 \times 10^{-5}$ and 2×10^{-7} moles/litre, which approximates the activities of manganese found in the spring water. The plots of Eh vs pH for locations 1, 2, 3, 4, 5, 6, 7, 9, and 10 (see Fig. 4) fall entirely within the field of free Mn^{+2} for the activities of manganese measured, but there is an obvious trend toward higher oxidation potentials and higher pH's from spring orifices downstream to locations at which manganese is observed to precipitate (locations 1, 2, 3, 9, and 10). Therefore, either manganese is precipitating as MnO_2 or Mn_2O_3 and the measured Eh-pH values are invalid, or manganese is precipitating as an unknown oxide that is stable at lower Eh-pH conditions. Both cases are possible; the absolute validity of field Eh readings is generally assumed to be doubtful (Garrels, 1960), but the existence of hydrous manganese oxides other than MnO_2 and Mn_2O_3 is suggested by X-ray studies.

The latter case is supported by the Eh readings obtained in bottom muck, both those in situ (see Fig. 5), and those of samples stored six months free of the atmosphere (see Fig. 6). Whereas some values plot in the field of stable MnO_2, most locations at which manganese is obviously precipitating plot outside the stable fields of MnO_2 and Mn_2O_3. Again the high stability of these readings in bottom muck increases one's confidence in their validity. Consequently, it is proposed that one or more hydrous oxides of manganese, which require lower Eh-pH conditions than MnO_2 and Mn_2O_3 for stability, constitute the major wad minerals.

Other Constituents

The cations Ca^{+2}, Mg^{+2}, Na^{+}, and K^{+}, and the anions SO_4^{-2} and Cl^{-} constitute the major remaining ionic species of the system. Other trace elements account for less than 0.4 per cent of the ionic concentrations. Probably any noticeable change in the concentrations of the minor constituents can be attributed to adsorption by electrically charged iron and manganese colloidal precipitates, or, in the case of volatiles, to equilibration with the atmosphere.

SUMMARY AND CONCLUSIONS

Iron is precipitated immediately on contact of the spring water with the atmosphere, and manganese is deposited farther downstream under higher Eh-pH conditions, suggesting that the redox potential, combined with the hydrogen ion activity, is the major mechanism of precipitation. The removal of iron and manganese from solution has negligible effect on Eh and pH conditions of the system, owing to their relatively low mole fraction of the ionic concentration. The oxidation potential is increased by thorough mixing of the water with atmospheric oxygen, and the pH is increased by dissociation of the

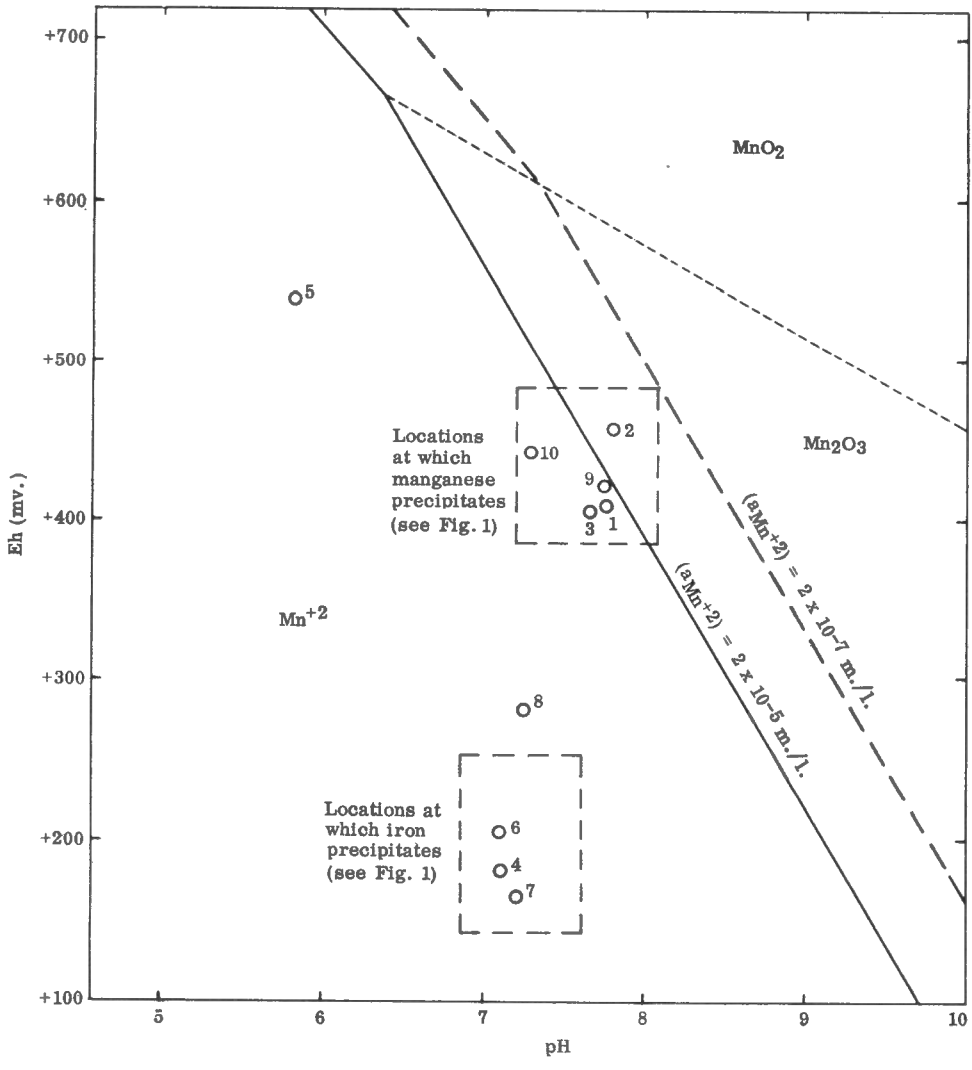

Location	$(a_{Mn^{+2}})$ m./l.	Location	$(a_{Mn^{+2}})$ m./l.
1	0.11×10^{-5}	6	2.2×10^{-5}
2	0.06×10^{-5}	7	2.0×10^{-5}
3	0.07×10^{-5}	8	—
4	2.0×10^{-5}	9	0.22×10^{-5}
5	0.02×10^{-5}	10	0.89×10^{-5}

Activities of Mn^{+2} for locations plotted above

GSC

Figure 4. Plot of Eh-pH values for free water with respect to the stability fields of MnO_2 and Mn_2O_3 at 10°C.

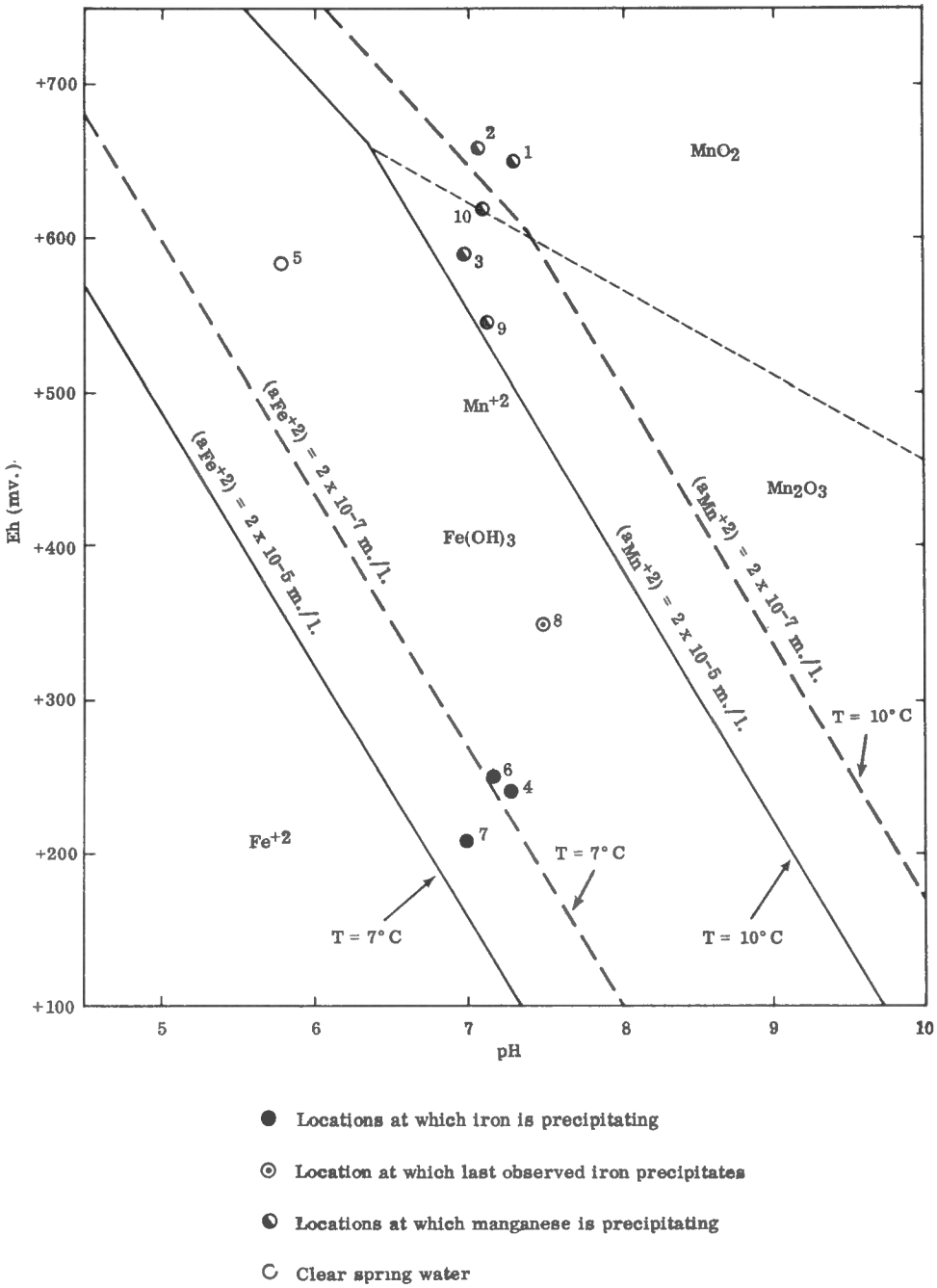

Figure 5. Plot of Eh-pH values for bottom muck in situ

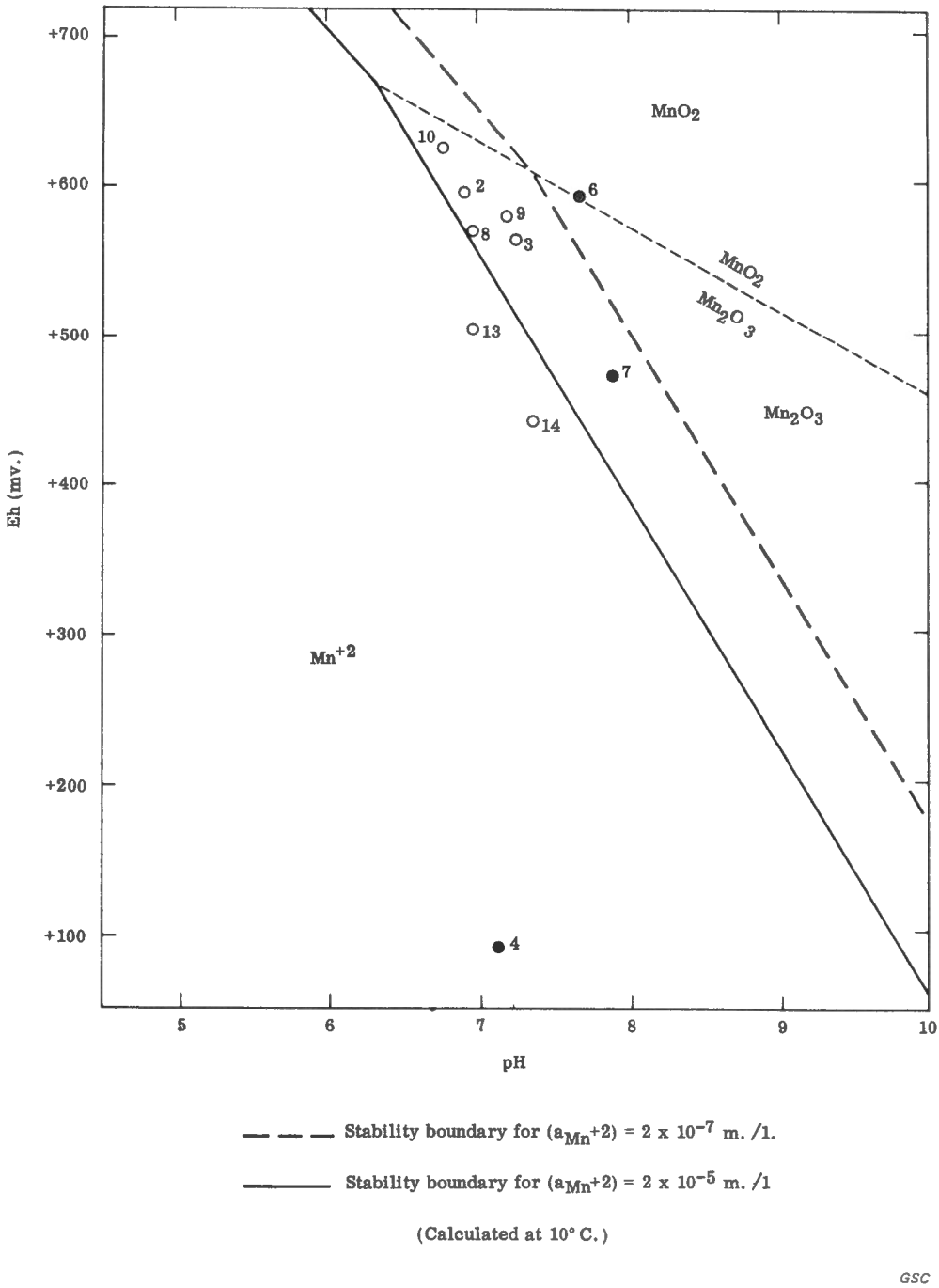

Figure 6. Plot of Eh-pH values for bottom muck stored free of the atmosphere for six months

bicarbonate ion, which is supersaturated at surface conditions, and tends toward equilibrium with CO_2 in the atmosphere. Other constituents perform no important role other than to increase the ionic concentrations.

Iron is probably carried in solution mainly as the free divalent ion Fe^{+2}, which oxidizes and hydrolyzes to colloidal $Fe(OH)_3$, as indicated by chemical observations and calculations, and by physical appearances. Manganese, also probably transported chiefly as the free divalent ion Mn^{+2}, is precipitated as an amorphous oxide under the high Eh conditions attained farther downstream after thorough mixing with the atmosphere. Neither the chemical nor mineralogical composition of the black precipitate has been determined by chemical or X-ray methods owing to its iron impurities and apparent amorphous state. The Eh-pH conditions at the locations of precipitation of manganese are not suitable for the stable existence of either MnO_2 or Mn_2O_3. Probably the precipitate is a hydrous manganese oxide having both divalent and tetravalent components and a lower Eh-pH stability limit. These conclusions are based on the assumption that the recorded field measurements are valid, and that an organic mechanism is absent. It has not been possible to evaluate these assumptions. A rigorous treatment of the problem awaits the completion of further studies on the oxides and hydrates of manganese and their amorphous equivalents, in particular, their chemical compositions and thermodynamic properties.

REFERENCES

Boyle, R.W., Illsley, C.T., and Green, R.N.
1955: Geochemical investigation of the heavy metal content of stream and spring waters in the Keno Hill-Galena Hill area, Yukon Territory; Geol. Surv., Can., Bull. 32.

Buser, W., and Grütter, A.
1956: The Nature of manganese nodules; Schweig. Min. Petrogr. Mitt., vol. 36, pp. 49-62 (abstracted in Chem. Absts., vol. 51, p. 3383, 1957).

1958: Radiochemische Untersuchung an Festkörpern, IV. Isotopen- bzw. Ionen-Austausch an Manganknollen; Trabajos de la Tercera Reunion Internacional sobre Reactividad de los Solidos, vol. II, pp. 373-379, Madrid.

Garrels, R.M.
1960: Mineral equilibria at low temperature and pressure; Harper and Brothers, New York.

Goldberg, E.D.
1954: Marine geochemistry I: Chemical scavengers of the sea; J. Geology, vol. 62, pp. 249-265.

Goldberg, E.D., and Arrhenius, G.O.S.
1958: Chemistry of Pacific pelagic sediments; Geochimica et Cosmochimica Acta, vol. 13, pp. 153-212.

Hanson, G.
1932: Manganese deposits of Canada; Geol. Surv., Can., Econ. Geol. Ser. No. 12, pp. 72-77.

Harvey, H.W.
1960: The chemistry and fertility of sea water; Cambridge Univ. Press, Cambridge.

Klotz, I.M.
1950: Chemical thermodynamics; Prentice-Hall, Inc., Englewood Cliffs, N.J.

Krauskopf, K.B.
1957: Separation of manganese from iron in sedimentary processes; Geochimica et Cosmochimica Acta, vol. 12, pp. 61-84.

Latimer, W.M.
1952: Oxidation potentials; Prentice-Hall, Inc., New York.

Palache, C., Berman, H., and Frondel, C.
1944: The system of mineralogy (Dana) Volume I; John Wiley and Sons, Inc., London.

Ramdohr, P.
1959: The manganese ores; Internat. Geol. Rev., vol. 1, No. 10, pp. 52-72.

Sandell, E.B.
1959: Colorimetric determination of traces of metals; Interscience Publishers, Inc., New York.

Savage, W.S.
1936: Transportation and deposition of manganese: Econ. Geol., vol. 31, pp. 278-298.

Smith, G.F., McCurdy, W.H., and Diehl, H.
1952: The colorimetric determination of iron in raw and treated municipal water supplies by use of 4, 7-Diphenyl-1, 10-Phenanthroline; Analyst, vol. 77, pp. 418-422.

Smitheringale, W.V.
1929: Notes on etching tests and X-ray examination of some manganese minerals; Econ. Geol., vol. 24, pp. 481-505.

Thomas, J.F.J.
1961: Chemical quality of spring waters from a bog near Dawson Settlement, Albert Co., N.B., 1961; Mines Branch, Dept. Mines Tech. Surv., Ottawa, Mineral Processing Division Test Report MPT 61-113.

Uglow, W.L.
1920: Bog manganese deposits, Dawson Settlement, Albert County, N.B.; Munition Res. Comm., Canada, pp. 65-88.

Zapffe, C.
1931: Deposition of manganese: Econ. Geol., vol. 26, pp. 799-832.

APPENDIX I

CALCULATION OF P_{CO_2} OF SPRING WATER

Assuming that the alkalinity of the water in the pH range 3 to 5 is due only to CO_3^{-2} and HCO_3^-, then

$$\text{carbonate alkalinity} = 2\ CO_3^{-2} + HCO_3^-.$$

From the dissociation of $CO_2 + H_2O$ and HCO_3^-,

$$K_1 = \frac{(a_{HCO_3^-})\ (a_{H^+})}{(a_{CO_2})\ (a_{H_2O})},$$

and

$$K_2 = \frac{(a_{CO_3^{-2}})\ (a_{H^+})}{(a_{HCO_3^-})}.$$

Therefore, carbonate alkalinity $= \frac{2(a_{HCO_3^-})\ K_2}{(a_{H^+})\ \gamma_{CO_3^{-2}}} + \frac{(a_{HCO_3^-})}{\gamma_{HCO_3^-}}$

$$= (a_{CO_2}) \left[\frac{K_1\ (a_{H_2O})}{(a_{H^+})}\right] \left[\frac{2\ K_2}{(a_{H^+})\ \gamma_{CO_3^{-2}}} + \frac{1}{\gamma_{HCO_3^-}}\right].$$

Also, $(a_{CO_2}) = \alpha P_{CO_2}$ where α is the solubility of CO_2 in water at a given temperature. Then,

$$P_{CO_2} = \frac{\text{Carbonate Alkalinity}}{\alpha \left[\frac{K_1\ (a_{H_2O})}{(a_{H^+})}\right] \left[\frac{2\ K_2}{(a_{H^+})\ \gamma_{CO_3^{-2}}} + \frac{1}{\gamma_{HCO_3^-}}\right]}$$

K_1, K_2, and α are obtained from Harvey (1960), and $\gamma_{CO_3^{-2}}$ and $\gamma_{HCO_3^-}$ are calculated using the Debye-Huckel equation,

$$\log \gamma = - A\ z^2 \sqrt{\mu}.$$

Ionic concentrations, μ, are calculated from the quantitative analyses of spring water, and (a_{H_2O}) is assumed to be unity.

APPENDIX II

CALCULATION OF Eh-pH STABILITY FIELDS

Temperature corrected Eh-pH relations are calculated from published standard ΔF and ΔH values by assuming ΔH and $\Delta S \neq f(T)$ for small temperature deviations (Garrels, 1960, p. 193). For example, the boundary between stable Fe^{+2} and stable $Fe(OH)_3$ may be calculated from the equation

$$Fe^{+2} + 3\,H_2O = Fe(OH)_3 + 3\,H^+ + e^-,$$

for which $\Delta F^\circ = 22.4$ Kcal and $\Delta H^\circ = +29.0$ Kcal at 25°C.

ΔF at temperature T may be calculated from

$$\Delta F = \Delta H - T\Delta S;\ \text{i.e.,}\ \Delta S = \frac{\Delta F - \Delta H}{-298.16} = 0.01544\ \text{Kcal/°K.}$$

Since iron is precipitating at T = 7°C ,

$$\Delta F_{7^\circ C} = 29.0 - 0.01544\,(280.16)$$
$$= 24.7\ \text{Kcal.}$$

Then, $Eh\ (\text{volts}) = E^\circ + \frac{RT}{n\mathcal{F}} \ln K;$

$$\text{i.e.,}\quad Eh = \frac{24.7}{1 \times 23.06} + \frac{0.00198\,(280.16)}{1 \times 23.06} \ln \frac{(aH^+)^3}{(a_{Fe^{+2}})},$$

or, $$Eh = 1.07 - 0.167\ pH - 0.0556 \log (a_{Fe^{+2}}).$$

This equation would form a surface in a three-dimensional diagram with Eh vs pH vs $(a_{Fe^{+2}})$, or a two-dimensional diagram with Eh vs pH for any desired $(a_{Fe^{+2}})$, if the temperature is assumed constant. Thus, for $(a_{Fe^{+2}}) = 2 \times 10^{-5}$ moles/litre,

$$Eh = 1.33 - 0.167\ pH.$$

In a similar manner, temperature corrected Eh-pH diagrams have been constructed for manganese oxides at a temperature of 10°C. (see Fig. 7):

$$Mn^{+2} + 2\,H_2O = MnO_2 + 4\,H^+ + 2\,e^-,$$
$$Eh = 1.24 - 0.1124\ pH - 0.0281 \log (a_{Mn^{+2}})$$
$$2\,Mn^{+2} + 3\,H_2O = Mn_2O_3 + 6\,H^+ + 2\,e^-,$$
$$Eh = 1.48 - 0.169\ pH - 0.0562 \log (a_{Mn^{+2}})$$
$$Mn_2O_3 + H_2O = 2\,MnO_2 + 2\,H^+ + 2\,e^-,$$
$$Eh = 1.02 - 0.0562\ pH$$

The significance of the phase boundaries as constructed above may be illustrated by the following example. A solution,

essentially devoid of dissolved oxygen and closed from the atmosphere, has a constant pH of 7 and temperature of 10°C , and an initial Eh of + 200 mv. (point A, Fig. 7), and contains 2×10^{-5} moles/l. each of iron and manganese.

At point A, the system is well within the stability fields of both Fe^{+2} and Mn^{+2} for activities of 2×10^{-5} moles/l. Therefore dissolved iron and manganese are the stable states.

However, by opening the system to the atmosphere, 3.58×10^{-4} moles/l. of oxygen may be dissolved in an aqueous solution at 10°C (Harvey, 1960). Under this condition, the oxidation potential of the system would reach point D:

$$O_2 + 2\,H_2O + 4\,e^- = 4\,OH^-$$

$$Eh = \frac{\Delta F}{4 \times 23.06} + \frac{0.059}{4} \log \frac{(a_{O2})}{(a_{OH^-})^4}$$

where ΔF 25°C = 41.1 Kcal., $(a_{O_2}) = 3.58 \times 10^{-4}$ moles/l., and $(a_{OH^-}) = 10^{-7}$ moles/l.

i.e., $$Eh = \frac{41.1}{4 \times 23.06} + \frac{0.059}{4} \log \frac{(3.58 \times 10^{-4})}{(10^{-7})^4}$$

$$= 0.81 \text{ volts.}$$

However, in proceeding from point A to D, the boundaries of both Fe^{+2} - $Fe(OH)_3$ and Mn^{+2} - Mn oxide will be crossed, and it is apparent that as the oxidation potential is gradually increased by the dissolution of atmospheric oxygen, the Fe^{+2} - $Fe(OH)_3$ boundary will be traversed before the Mn^{+2} - Mn oxide boundary. That is, iron will become unstable before manganese, and precipitation of iron as $Fe(OH)_3$ will precede precipitation of manganese as an oxide.

In detail, iron will begin to precipitate as soon as the Fe^{+2} - $Fe(OH)_3$ boundary for $(a_{Fe^{+2}}) = 2 \times 10^{-5}$ moles/l. is crossed (point B). As further atmospheric oxygen dissolves and iron precipitates, $(a_{Fe^{+2}})$ will simultaneously decrease, and the Fe^{+2} - $Fe(OH)_3$ boundary will migrate in the direction of the Mn^{+2} - Mn oxide boundary (for example, see the boundary for $(a_{Fe^{+2}}) = 2 \times 10^{-7}$ moles/l.).

At point C, nearly all iron will have precipitated, and manganese, now unstable as Mn^{+2} for $(a_{Mn^{+2}}) = 2 \times 10^{-5}$ moles/l., begins to precipitate as Mn_2O_3 according to the constructed Eh-pH diagram. As in the case of iron, the Mn^{+2} - Mn_2O_3 stability field boundary migrates toward higher Eh-pH values as further oxygen is dissolved and manganese is precipitated simultaneously. Note that at

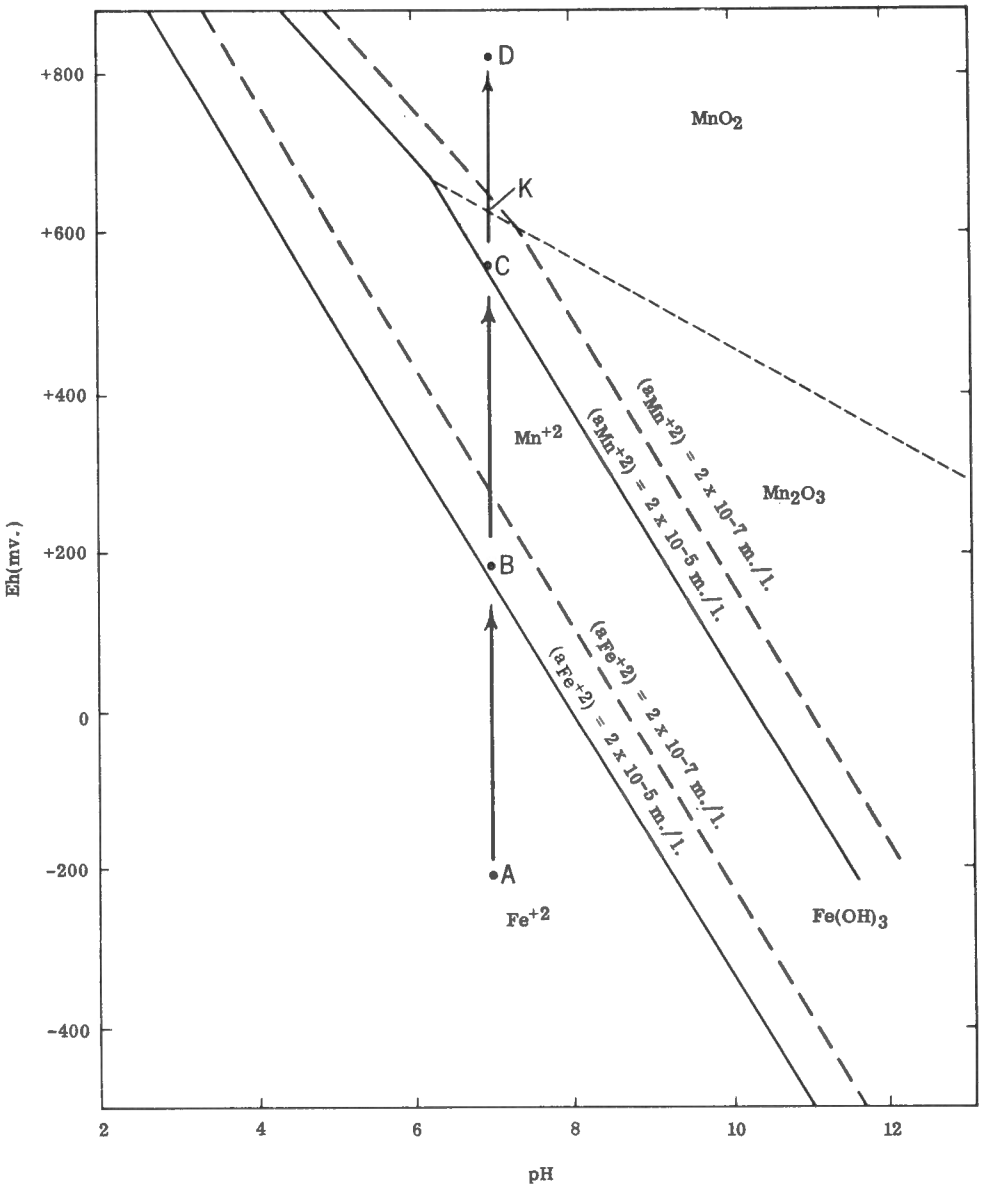

Figure 7. Stability fields of $Fe(OH)_3$, MnO_2, and Mn_2O_3

point K, manganese precipitates as MnO_2, and previously precipitated Mn_2O_3 now either undergoes further oxidation to MnO_2 or continues to exist as metastable Mn_2O_3.

ROGER DUHAMEL, F. R. S. C.
QUEEN'S PRINTER AND CONTROLLER OF STATIONERY
OTTAWA, 1963
Price 35 cents Cat. No. M44-63/42